Anisotropic Diffusion and Morphology in Perfluorosulfonate Ionomers Investigated by NMR

Jing Li, Kyle G. Wilmsmeyer, and Louis A. Madsen*

Department of Chemistry and Macromolecules and Interfaces Institute, Virginia Polytechnic Institute and State University, Blacksburg, Virginia 24061

Received September 16, 2008; Revised Manuscript Received November 14, 2008

ABSTRACT: Anisotropy in ionomer membranes represents a powerful interaction for modulating properties such as mechanical moduli, thermal expansions, and small molecule transport, all tunable via controlled processing. We observe uniform hydrophilic channel alignment in three perfluorosulfonate ionomer membrane types, quantified by ^{2}H NMR spectroscopy of absorbed D_2O molecules. Our measurements show biaxial or uniaxial in-plane alignment for extruded membranes, but uniaxial through-plane alignment for dispersion-cast membranes, and further demonstrate affine swelling with both water uptake and thermal expansion. In order to correlate alignment data with a quantity relevant to proton transport, we measure the anisotropy of water self-diffusion using pulsed-field-gradient NMR along different membrane directions. Extruded membranes with stronger alignment exhibit 18% faster in-plane diffusion than through-plane diffusion, while diffusion anisotropy is minimal for weakly aligned membranes. These results should lead to a more quantitative understanding of and control over membrane properties via manipulation of molecular order.

I. Introduction

Perfluorosulfonate ionomers have diverse applications in polymer electrolyte membrane (PEM) fuel cells, reverse-osmosis water desalinization membranes, and "artificial muscle" polymer actuators.[1] In most applications, small polar or ionic mobile solutes such as water, ionic liquids, lithium, or protons transport through the membrane plane via a nanometer-scale hydrophilic phase. Proton conductivity measurements on some of these ionomers have shown substantial directional anisotropy, but with limited quantitative understanding. Ma et al.[2] have reported anisotropic conductivity for in-plane relative to through-plane directions in hot-pressed Nafion 117 (N117). Cable et al.[3] have also demonstrated in-plane conductivity anisotropy in uniaxially oriented N117 and correlated this with SAXS measurements. Our previous brief study[4] showed distinct oriented morphologies in two Nafion membranes processed under different conditions via ^{2}H NMR spectroscopy. Thus, transport anisotropy is undoubtedly influenced by the oriented morphology. Ionic polymer features such as crystallinity and ionic aggregate size and dimensionality have been measured using XRD,[5−10] NMR,[4,11−13] and electron microscopy,[14] but links between orientation and transport require deeper and more quantitative investigation.

We aim to quantitatively assess both morphological structure and transport properties of these membranes in order to build models for membrane behaviors and to tailor membranes to suit diverse applications. Here we present a more complete picture of anisotropy by incorporating a third membrane type (extruded Nafion 117) and conducting detailed multiaxis diffusion measurements using pulsed-field-gradient NMR. We observe clear diffusion anisotropy in the most oriented membrane (extruded Nafion 112), which clearly correlates with molecular anisotropy (^{2}H NMR) measurements. We further map out the sensitive dependence of ^{2}H NMR spectral splitting as a function of water uptake, temperature, and membrane type, where we confirm affine swelling of these membranes under all conditions.

A. Measurements of Hydrophilic Channel Anisotropy. Fuel cell membranes normally operate at 10−40 wt % water uptake to maximize proton conductivity. Protons conduct in the acidified bath of water contained in the ion-lined hydrophilic channels, which provides a low activation energy environment for transport. Several models based on XRD scattering curves describe this hydrophilic phase as a network of ion clusters and hydrophilic channels that grow in size with water uptake.[5,6,8−10] Induced alignment of membrane polymer chain and ion clusters are studied by XRD[3,6] showing a hierarchical scale of structure. In this work, we investigate the membrane hydrophilic channel alignment order using deuterated probe molecules, specifically D_2O to replace the usual H_2O present in these membranes. This method is widely used in liquid crystal and conventional polymer systems.[15] Doping a simple deuterated probe molecule into an ordered liquid or solid provides easy access to the orientational order parameter $\boldsymbol{S}$ (a.k.a., the Hermann's orientation function) as well as to higher order tensorial orientation properties.[15] This method provides quantitative, although relative, measures of $\boldsymbol{S}$ and other order parameters, and these can be extremely useful in characterizing ordered phase behavior, temperature dependencies, and phase symmetries. It may be conducted on almost any NMR spectrometer and does not require complicated sample mounting or sectioning for film cross sections to interact with, e.g., an X-ray or neutron beam. Study of perfluorosulfonate ionomers benefits greatly from application of this method since they heavily absorb water, which we replace with D_2O. Compared to scattering techniques,[6] which reveal the orientational order of the hydrophobic Nafion amorphous/crystalline backbone and hydrophilic ionic clusters, this ^{2}H NMR method focuses simply on the orientational order of the hydrophilic channels to which the D_2O probe molecules have access. As the probe molecules diffuse in the hydrophilic channels of the membranes, they acquire partial ordering due to biased rotations, collisions, and librations of these D_2O probe molecules, including collisions with the quasi-cylindrical channel walls. This temporal and spatial ensemble average gives rise to "inherited" orientational order of the deuterated probe solute molecules as they interact with an anisotropic matrix.[15,16] The actual average order of the probe molecules is reduced compared to the order of the host channels by a scaling factor. Such a "pseudonematic interaction"[17] is manifested in the quadrupole splitting of the probe molecules. In nanophase-separated ionomers such as Nafion, which consist of interconnected voids,

* Corresponding author. E-mail: lmadsen@vt.edu.

10.1021/ma802106g CCC: $40.75
Published on Web 12/10/2008

lamellae, or channels, one observes a single deuterium doublet spectrum (splitting) only if there is alignment of these channels macroscopically over the membrane. Orientational distributions of domains larger than the diffusion length of D_2O on the $1/Q_pS$ time scale ($\sim$1 μm and $\sim$1 ms, respectively, see eq 1) manifest as superpositions of deuterium doublet spectral components, which will thus broaden and provide additional structure to the observed spectrum.

Residual quadrupole splittings $\Delta\nu_Q$ of the water deuterons report on $\boldsymbol{S}$ via[17]

$$\Delta\nu_Q = Q_p \boldsymbol{S} P_2(\cos\theta) = Q_p \rho \boldsymbol{S}_{matrix} P_2(\cos\theta) \qquad (1)$$

where Q_p is the quadrupole coupling constant ($\sim$260 kHz), and $\boldsymbol{S} = \langle P_2(\cos\chi)\rangle$ is the ensemble average over the second Legendre polynomial with χ the angle between a particular OD bond axis and the alignment axis of the material. θ defines the angle between the material alignment axis and the spectrometer magnetic field $\mathbf{B_0}$. We are generally more interested in the order parameter of the channel network matrix itself, which can be expressed as $\boldsymbol{S} = \rho\boldsymbol{S}_{matrix}$, where $\boldsymbol{S}_{matrix} = \langle P_2(\cos\alpha)\rangle$ is the ensemble average over the second Legendre polynomial with α the angle between a particular channel axis and the alignment axis of the material; ρ is the scaling factor determined by the interaction between the probe molecule and the host matrix. Usually, ρ is fixed for a given probe−matrix system and is relatively insensitive to temperature for liquid crystal or conventional homogeneous polymer systems.[17,18] Equation 1 describes a uniaxial system. In the case of an isotropic system, $\mathbf{S}$ would average to zero; hence, a single ^{2}H peak with no splitting is observed. In the case of nonuniaxial alignment, we may replace $\boldsymbol{S}P_2(\cos\theta)$ in eq 1 with appropriate tensorial equations to extract various asymmetry parameters.

B. The Role of Water Uptake. Water uptake in ionomer-based membranes, affected by humidity, strongly influences ionomeric fuel cell[19] and mechanical actuator performance.[20,21] Previous studies using residual ^{2}H NMR quadrupolar interactions in perfluorosulfonate ionomers[11−13] usually adjust water uptake by controlling relative humidity (RH) and also leave substantial dead volume in the NMR sample cells. While modulating RH is convenient from an engineering and end-use standpoint, the downside is that moisture can still leave the membrane due to evaporation hence actual water uptake is not steady. For critical processes within the membrane, water uptake is the relevant variable influencing transport and chemical properties, while RH only affects surface properties and, variably, the amount of water uptake. Furthermore, the water uptake−humidity relationship is not the same for different membranes. According to our observations, the same membrane that is subjected to different thermal treatments will uptake water differently at a given humidity. We note that the quadrupole splitting, and indeed relevant transport parameters such as the diffusion constant and proton conductivity, strongly depend on the water uptake. An unsteady water uptake level will lead to inconsistent NMR quadrupole splitting measurements as well as water self-diffusion results discussed in the second part of this paper, which makes quantitative analysis difficult. In this work for both the ^{2}H NMR and the water self-diffusion studies, we use sealed and equilibrated low-dead-volume sample cells that provide exquisitely reproducible and quantifiable results. In addition, we take advantage of the quantitative nature of NMR measurement to verify the water uptake through comparison of NMR signal intensity with gravimetric data. In our initial study,[4] we found uniform order in two commercial Nafion membranes using our simple and quantitative ^{2}H NMR method. In this paper, we present detailed orientational order measurements and water transport properties (self-diffusion) in three leading Nafion membranes. We demonstrate that this channel alignment is uniform over these films but has drastically different properties for different membrane types. We report the dependencies of ^{2}H quadrupole splitting on D_2O uptake and temperature, confirming that thermal swelling of these membranes is rigorously affine. Quantifying this order allows for feedback on anisotropic conductivity in these ionomer membranes.

Table 1. Nafion Membrane Types Investigated

type of Nafion	membrane thickness (μm)	processing method
N112	50	extruded
NRE212	50	dispersion cast
N117	175	extruded

C. Diffusion Anisotropy in Ionomer Membranes. The transport properties of water and ions in Nafion are commonly measured by pulsed-field-gradient (PFG) NMR self-diffusion experiments.[22,23] Saito et al. suggested[17] that protons in the membranes transport by the Grotthuss hopping mechanism[24] and the larger ions (Li^+, Na^+, etc.) by the vehicle mechanism.[25] Zhang et al. studied tortuous self-diffusion behavior of commercial and recast Nafion[26] and observed a dependence of apparent diffusion coefficient over a range of diffusion times, attributing this to the water interaction with the ionic clusters. This measurement provides intrinsic information on the translational motion of water molecules and free or hydrated protons/ions in the membranes. Compared to conductivity measurements, which report both isotropic[2,3,27,28] or anisotropic[2,3] conductivity in Nafion, an as yet unsettled topic in literature, the PFG-NMR self-diffusion measurement is a noncontact technique that eliminates the complication and variation of electrode interfaces and does not require complex mathematical models to convert and compare in-plane vs through-plane conductivity. For isotropic systems, the diffusion coefficient measured in the PFG direction represents the overall 3-dimensional diffusion behavior. For anisotropic systems, the diffusion coefficient obtained will depend on the relative orientation of the material with respect to the NMR field gradient direction. Fechete et al.[29] detected small diffusion anisotropy of toluene in uniaxially compressed natural rubber samples using NMR self-diffusion. Rollet et al.[30] used radio tracer and NMR techniques to demonstrate transport anisotropy of ions in sulfonated polyimide ionomer membranes where a faster in-plane over through-plane diffusion was observed. We apply the PFG diffusion method to describe the transport anisotropy in three commercial Nafion types by placing the H_2O swollen membrane at three orthogonal directions with respect to the PFG direction in order to correlate morphological orientation and transport properties. Our diffusion anisotropy results correlate well with our orientational order measurements, providing a link between channel ordering and molecular transport.

II. Experimental Section

A. Materials. Nafion 112 and Nafion 117 (extruded) and Nafion NRE212 (dispersion-cast) membranes, all nominally 1100 equiv weight (EW) per sulfonate group, were obtained from E.I. DuPont (Wilmington, DE) in acid form. The membrane thickness and processing method are listed in Table 1. Deuterium oxide was obtained from Cambridge Isotope Laboratories, Inc. (Andover, MA) at 99.9% purity. Membranes and solvents were used as received.

B. Orientational Order Measurements. All NMR experiments were performed on a Bruker Avance III WB NMR spectrometer (Bruker-BioSpin, Billerica, MA) at a magnetic field of 9.4 T, corresponding to a ^{1}H frequency of 400 MHz and a ^{2}H frequency of 61.4 MHz. A single channel detection static solids probe with a 10.7 mm inside diameter horizontal solenoid coil was used for ^{2}H spectroscopy experiments.

Extruded Nafion membranes were cut into 6 × 6 mm pieces with one edge along the extrusion striate. The orientation was

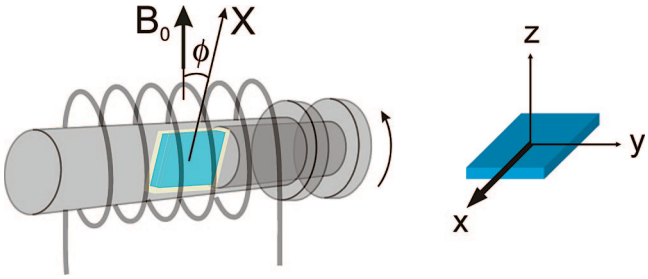

Figure 1. Schematic diagram of the sample cell and definition of membrane directions. The sample cell contains a slit for the membrane stack (blue block) and a pressure fit piston cap to seal the container and allow the sample to equilibrate with very low dead volume (<20%). The three axes in the rectangular blue block indicate three membrane principal directions, where the membrane **z**-axis is perpendicular to the plane. For the extruded membrane, **x** is the extrusion direction as indicated by the thicker arrow. For dispersion cast membranes, **x** is an arbitrary in-plane direction. **y** is in the membrane plane perpendicular to **x**. The entire cylindrical cell is rotated inside the solenoid rf coil, and thus the angle ϕ between membrane in-plane direction **x** axis and the magnetic field can be varied.

confirmed by polarizing microscopy (Meiji Technology MX9430, Japan). Dispersion-cast Nafion membranes were cut into the same size with an orientation relative to the film sheet edges. Ten pieces were stacked in exactly the same orientation to enhance NMR signal. The stacks of dry membranes were placed in a 40 °C oven for 5 h, weighed, then loosely wrapped with Teflon pipe seal tape, and soaked in D_2O for at least 1 week. The maximum D_2O uptakes, expressed in wt %, were measured by the weight gain versus the weight of the dry membranes. The wt % of unsaturated membranes was measured by the partially swollen membrane weight and confirmed with relative NMR signal intensity. Error in this uptake wt % is ±10% of the absolute water uptake; e.g., at 20 wt % uptake the error is ±2 wt %, and at 5 wt % the error is ±0.5 wt %. The NMR probe was tuned and matched to ensure the shortest 90° pulse time. Before NMR experiments, the membrane stacks were wrapped with Teflon tape and LDPE plastic wrap and sealed in a Delrin sample cell as shown in Figure 1, followed by equilibration for 3 h before taking measurements. The sample cell can be rotated in the NMR coil casing, using a goniometer to accurately adjust orientation of the sample cell to ±1.5° accuracy.

^{2}H NMR experiments utilized a simple free induction decay (FID) acquisition following a single pulse of 4 μs ($\pi/2$ pulse = 6 μs) and a repetition time of 0.7 s for 256 or 1024 scans. The deuterium quadrupole splittings were extracted from the data by fitting each spectrum with two Lorentzian peaks using NutsPro software (Acorn NMR Inc., Livermore, CA). A calibration curve of splitting versus wt % was established for each sample by running consecutive NMR experiments with the sample cell cap partially removed, allowing D_2O to slowly evaporate from the membranes over a period of 2−3 days. Peak areas, along with gravimetric calibration data, were used to calculate wt % of actual D_2O in membranes as a function of time. Angle between the membrane sample cell and the static magnetic field was varied in 15° steps from 0° to 90°. At room temperature, T_1 values are 200 ms for saturated membranes and 40 ms for nearly dry membranes.

C. Diffusion Coefficient Measurements. Self-diffusion coefficients of water (^1H_2O) in membranes were measured using the 400 MHz Bruker Avance III WB NMR equipped with a single axis diffusion probe having a maximum gradient of 2982 G/cm. Pulsed-gradient stimulated echo (PGSTE) experiments were performed at 25 °C. Temperature was calibrated using 100% ethylene glycol standard to an accuracy of 0.2 °C. The gradient constant was calibrated by measuring the diffusion coefficient of 1% H_2O/D_2O doped with 0.1 mg/mL $GdCl_3$ to a literature value of 1.872×10^{-9} m^2/s at 25 °C.

The free diffusion NMR signal attenuation is described by the following equation:[31]

$$I = I_0 e^{-D\gamma^2 g^2 \delta^2 (\Delta - \delta/3)} = I_0 e^{-Db} \quad (2)$$

where I is the spin−echo signal intensity, I_0 is the signal intensity at zero gradient, γ is the gyromagnetic ratio of the probe nucleus (rad s^{-1} T^{-1}), δ (s) is the duration of the field gradient pulse with magnitude g (T m^{-1}), D is the self-diffusion coefficient of water in the membranes, and Δ is the duration between the leading edges of the two gradient pulses. b is commonly known as the Stejskal−Tanner parameter[31] in clinical literature and also sometimes has the label Q. The signal intensity I is measured as a function of g to deduce the diffusion coefficient of water in the membranes. For each experiment, a range of Δ values were used to evaluate the diffusion coefficients. In order to measure diffusion anisotropy, membrane samples were trimmed the same way as for the ^{2}H NMR experiment, soaked in H_2O for more than 48 h, and water uptake measured by gravimetry after blotting the membrane to remove free water. For in-plane diffusion, the sample stacks were loaded into a sample cell similar to Figure 1, which is made of Teflon and can fit vertically into an 8 mm double resonance saddle-shape RF coil. For through-plane diffusion, another Teflon cell comprised of a cylindrical cavity (6.5 mm i.d., 8 mm o.d.) and a piston cap was used. In the latter cell, the same sample can be placed in the center of the 8 mm RF coil with spectrometer magnetic field $\mathbf{B}_0$ direction normal to the membrane surface. An equilibration time of 3 h in the sealed sample cell was allowed prior to diffusion measurements, based on a measured 1−2 h time to reach steady state when measuring ^{2}H spectra and diffusion constants. In terms of reproducibility among different experiments, allowing for uptake errors and using careful calibrations with known standards, we estimate an absolute accuracy of $D = \pm 3\%$. However, within a certain group of diffusion anisotropy experiments (as in for one membrane at different angles as in Figures 7 and 8), we estimate a tighter accuracy of $D = \pm 2\%$.

III. Results and Discussion

A. Orientational Order, Affine Swelling, and Morphological Models. Figure 2A shows NMR spectra as a function of Nafion 112 membrane angle ϕ with respect to $\mathbf{B}_0$, rotating about the membrane **y**-axis. Here, the membrane **x**-axis corresponds to the principal alignment direction, or "director", as it is the direction where maximum splitting occurred, so ϕ becomes θ in eqs 1 and 3 for N112. Because of the membrane biaxiality, and using an extension of eq 1, the quadrupole splitting follows a dependence given by[15,17,32,33]

$$\Delta\nu_Q = \frac{1}{2}\Delta\nu_0[3\cos^2\theta - 1 + \eta\sin^2\theta] \quad (3)$$

which we may use to fit splittings as a function of angle and wt % D_2O uptake, shown in Figure 2B. Here we note that the biaxiality parameter $\eta = 0.12 \pm 0.02$ is stable over hydration levels of 6−13 wt %, indicating that the degree and symmetries of alignment in these channels are stable vs hydration level. Further experiments using only the three **x**, **y**, and **z** directions of sample orientation[4] showed that this $\eta = 0.12$ is stable over at least a hydration level range of 4−20 wt %. Similar analyses for Nafion NRE212 are shown in Figure 2C, D. In Figure 2C,D the angle ϕ is defined as the angle between an (arbitrary) in-plane membrane direction **x** and the magnetic field direction $\mathbf{B}_0$. In this case, one can immediately notice from the rotation pattern that the principal alignment direction (director) is perpendicular to the membrane in-plane **x** axis, i.e., in the through-plane **z** axis direction. Therefore, the angle θ of eq 3 becomes $90° - \phi$ for NRE212. Figure 2D shows that dispersion-cast NRE212 exhibits uniaxial order ($\eta = 0$) over hydration levels of 5−20 wt %. Both results in Figure 2B, D clearly indicate affine swelling in these two Nafion membranes. We observe in Figure 2 that the zero $\Delta\nu_Q$ crossover angle $\theta_{\Delta\nu_Q} = 0$ is equal to the magic angle 54.7° since $\eta = 0$ for NRE212,

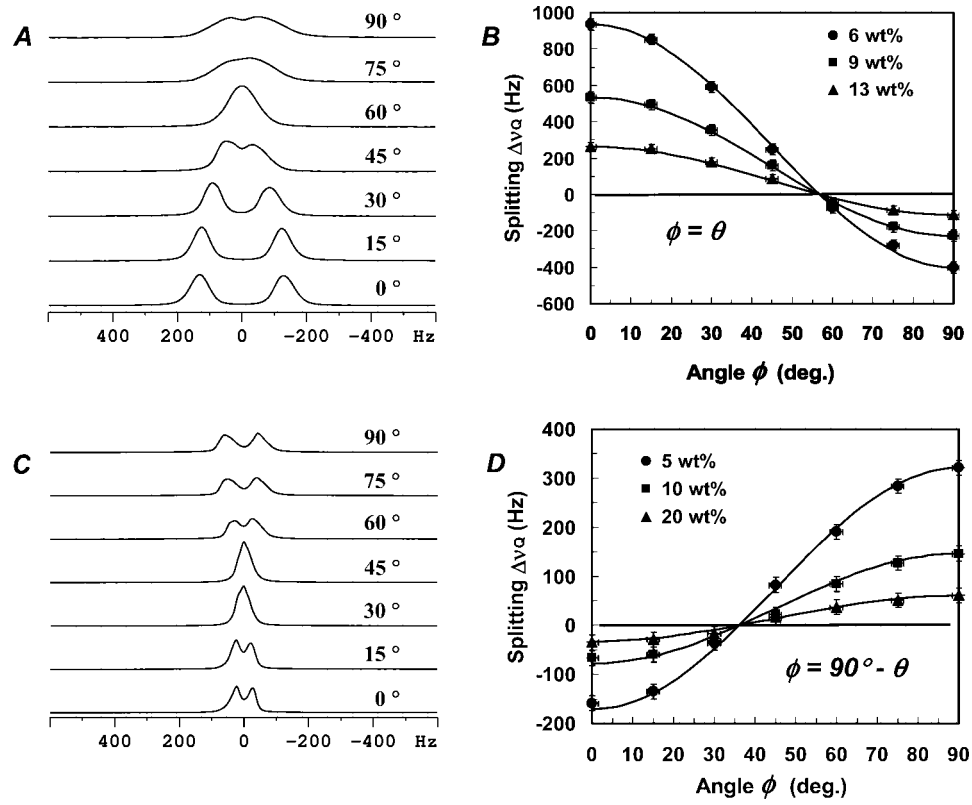

Figure 2. ^{2}H NMR spectra vs rotation angle for N112 (A) and NRE212 (C) with 13 wt % D_2O. (B) Plots of quadrupole splitting $\Delta\nu_Q$ vs angle ϕ of the extrusion direction relative to the spectrometer field $\mathbf{B}_0$ over a range of D_2O uptake in N112. Solid lines are fitted curves using eq 3, where $\theta = \phi$, and $\eta = 0.12 \pm 0.02$ provides best fits for all curves and is the only adjustable fit parameter after specifying $\Delta\nu_0$, the spectral splitting at $\phi = 0$. (D) Plots of quadrupole splitting $\Delta\nu_Q$ vs angle ϕ of the **x** (in-plane) direction relative to the spectrometer field $\mathbf{B}_0$ over a range of D_2O uptake in NRE212. Solid lines are fitted curves using eq 3, where $\theta = 90°-\phi$, and $\eta = 0$ provides best fits for all curves and is the only adjustable fit parameter after specifying $\Delta\nu_0$, the spectral splitting at $\phi = 90$. The error estimate for η based on all our data fits is ± 0.02.

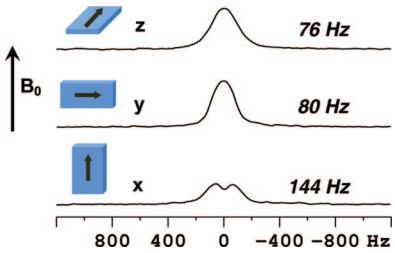

Figure 3. Room temperature ^{2}H NMR spectra for N117 at 7 wt % D_2O uptake. The rectangular blocks in blue indicate different membrane directions (**x, y, z**) lying parallel to the spectrometer $\mathbf{B}_0$ field. The arrows indicate the extrusion direction. The quadrupole splitting values $\Delta\nu_Q$ at right result from nonlinear least-squares fits to each spectrum.

while $\theta_{\Delta\nu_Q} = 0$ for N112 is 56.4°, larger than the magic angle due to the biaxiality $\eta = 0.12$. This provides an additional indication of biaxiality for N112. Furthermore, by comparing the quadrupole splittings of the two membranes at the same hydration level as shown in Figure 2A, C, one finds that the quadrupole splitting and thus the orientational order parameter S is 2.5 times larger in N112 than in NRE212. Thus, this morphological alignment, in the through-plane direction, shows substantial room for improvement over as-received NRE212, which would be highly desirable for operating fuel cells and other ionomer-based devices that depend on maximizing through-plane conductivity.

On the basis of the methods of our previous work,[4] we examined the ^{2}H NMR quadrupole splitting of extruded N117 at three orthogonal angles as shown in Figure 3. This provides adequate orientational information for up to second degree order (biaxial) by using $\eta = |\Delta\nu_Q^y - \Delta\nu_Q^z|/\Delta\nu_Q^x$. Figure 3 shows that order in N117 is uniaxial ($\eta = 0$) and along the extrusion direction to within experimental errors. The error in $\eta = \pm 0.04$ in this case is due to fitting errors of these spectra. We observe that the quadrupole splitting is dramatically smaller for N117 at 7 wt % (144 Hz) compared to N112 (936 Hz) at a similar uptake (6 wt %), as shown in Figure 2A. Both biaxial and uniaxial orders can sensibly arise from the extrusion processes inducing mechanical stress on the membranes. The smaller order in N117 likely results from the substantially smaller shear and extensional forces imparted on the much thicker N117 membrane (175 μm) relative to the N112 membrane (50 μm). We also find that for a given membrane the quadrupole splitting increases as the membrane D_2O uptake decreases as shown in Figure 2. This results from a stronger "pseudonematic interaction"[17] as average channel size is smaller (surface-to-volume ratio is larger) at low uptake, and D_2O molecules will experience more anisotropic interactions with the channel walls than with other D_2O molecules. In other words, the scaling factor ρ in eq 1 is larger at low D_2O probe molecule uptake. This dependence necessitates fine control of D_2O uptake when conducting these experiments. It also explains the lack of systematic splitting reported in previous studies,[11−13] most likely due to larger dead volume or temperature spreads over the sample cell and thus less control over water uptake.

Figure 4 depicts models for the channel morphologies in these membranes. In order to emphasize the alignment quality, these models are simplified descriptions of Nafion morphology, which could consist of interconnected channels, lamella, and clusters in three dimensions.[5] Recent work by Schmidt-Rohr and Chen strongly indicates randomly packed parallel cylindrical hydrophilic channels (diameter ~2.4 nm at 20 vol % H_2O).[10] Another study by Rollet et al. indicates cylindrically symmetric fibrillar bundles with similar ~2 nm diameter and a persistence length

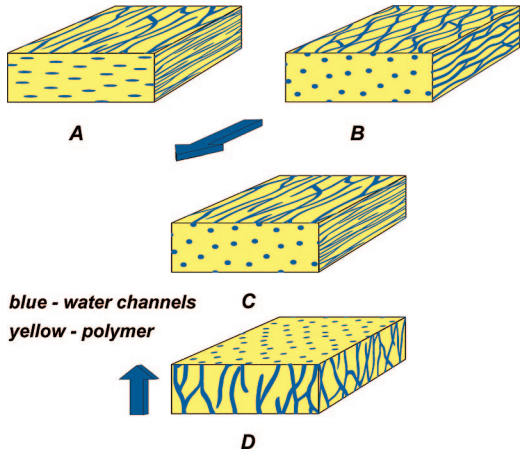

Figure 4. Proposed hydrophilic channel alignment models for N112 (A and B), N117 (C), and NRE212 membranes (D). (A) Biaxiality caused by ellipsoidal channels aligned along the extrusion direction (block arrow) in the membrane plane. (B) Biaxiality caused by cylindrical channels with directional anisotropy in the membrane plane relative to across the plane (zigzag character in film plane and perpendicular to extrusion direction). (C) Uniaxially aligned cylindrical channels in the membrane plane along the extrusion direction. (D) Uniaxially aligned cylindrical channels perpendicular to the membrane plane (block arrow). Arrow also indicates solvent evaporation gradient direction.

of ~100 nm.[8] Both of these models assert essentially well-defined walls and allow high water permeability. In all cases, the channels are strongly interconnected resulting in water percolation as shown by water self-diffusion results in section III.B of this paper. Parts A and B show two possible biaxial morphologies, consistent with our data, for the extruded N112 channel morphology. Part A depicts biaxial (elliptical) channels aligned uniaxially along the extrusion direction, while part B depicts uniaxial (cylindrical) channels aligned biaxially via larger local bends in-plane vs through-plane. Distinguishing between parts A and B requires further structural studies, e.g., microscopy and XRD with suitable modeling,[9,10] or further NMR diffusometry or relaxometry techniques we are exploring. A direct observation with electron microscopy on the nanometer scale features in water-swollen membranes is extremely challenging if not impossible. At present, we are working toward a model to reveal the relationship between probe molecule quadrupole splitting and channel order parameter S_{matrix} (see eq 1) by taking into account the shape and area of the channel cross section. Such a model could potentially resolve the difference between morphology A and B and would provide independent measures of ρ and S_{matrix}. Part C shows the morphology model for extruded N117, in which the hydrophilic channels have cylindrical shape and uniaxially align in the extrusion direction with minimal biaxiality. Part D shows the dispersion-cast NRE212 channel morphology, consisting of cylindrical channels aligned uniaxially across the plane of the film. This could include weak ordering (tilting) of bundles[8] through-plane with bundle long axis directions randomized in the plane. This through-plane alignment is likely formed during the casting process by solvent evaporating (flowing) in the direction normal to the membrane plane. The supporting substrate for the dispersion casting process may also induce order in the final membrane formed, as is commonly seen in liquid crystal surface alignment techniques.[34] Note that these models and our observations do not necessarily specify whether Nafion exhibits a cluster-network model[5] or quasi-cylindrical channel models[8,10] but do support cylindrical (biaxial for N112) alignment symmetry.

Parts A and B of Figure 5 summarize the temperature-dependent ^{2}H quadrupole splitting for N112 and NRE212 at 20 wt % D_2O uptake, respectively. First we notice that the splittings

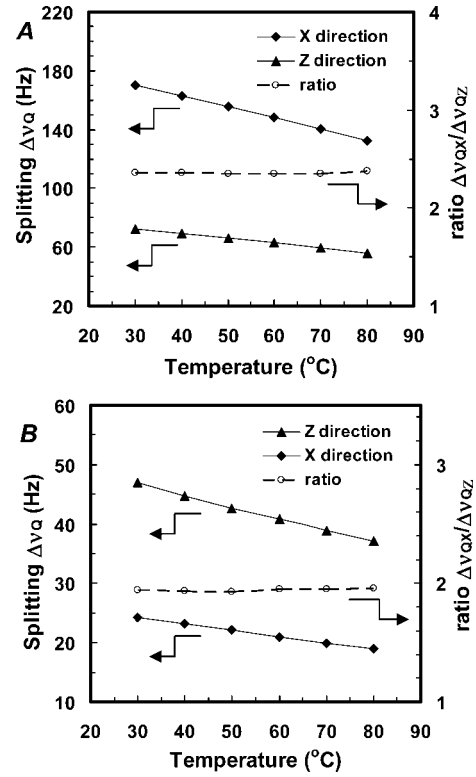

Figure 5. Quadrupole splittings $\Delta\nu_Q$ vs temperature at 20 wt % D_2O uptake for N112 (A) and NRE212 (B) in two reference directions as defined in Figure 1. Solid symbols represent $\Delta\nu_Q$ measurements, while open circle and dotted lines represent the ratios between splittings at these two directions.

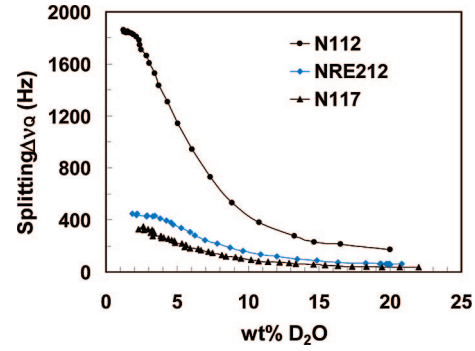

Figure 6. Plots of quadrupole splittings $\Delta\nu_Q$ vs D_2O uptake for N112 (black circle), NRE212 (blue diamond), and N117 (black triangle) with their maximum alignment direction (splitting maximum) parallel to magnetic field $\mathbf{B}_0$. These curves allow for direct comparison of order in different membranes and provide another method of measuring water uptake using $\Delta\nu_Q$.

decrease as temperature increases, which can be explained by the thermal expansion of the hydrophilic channels that leads to a weaker "pseudonematic interaction"[17] between the D_2O molecule and the channel walls and hence a smaller ensemble average S in eq 1 and smaller quadrupole splitting. The other obvious observation is that the ratios between the splitting at two reference angles are steady in temperature ranging from 25 to 80 °C, indicating the biaxiality/uniaxiality in respective systems does not change upon heating; i.e., the thermal expansion of the two membranes is affine. We note that in our first experiments using poorly sealed sample cells (a capped 18 cm long 10 mm NMR tube with membrane held up by half-cylindrical Teflon spacers) we observed nearly flat but slightly increasing splittings with temperature. In view of our Figure 6 results, this was undoubtedly due to water evaporation during

Table 2. ^{2}H NMR Quadrupole Splittings and Diffusion Coefficients in Three Membrane Directions for Various Nafion Types

D_2O/Nafion quadrupole splitting	$\Delta\nu_Q^x$ (Hz)	$\Delta\nu_Q^y$ (Hz)	$\Delta\nu_Q^z$ (Hz)
N112 at 6 wt %	936	−528	−401
NRE212 at 5 wt %	−159	−162	321
N117 at 7 wt %	144	−80	−76
H_2O/Nafion self-diffusion	D_{xx} ($\times 10^{-10}$ m^2/s)	D_{yy} ($\times 10^{-10}$ m^2/s)	D_{zz} ($\times 10^{-10}$ m^2/s)
N112 at 8 wt %	2.88	2.47	2.44
N112 at 22 wt %	5.48	4.81	4.64
NRE212 at 20 wt %	5.83	5.86	5.58
N117 at 21 wt %	6.11	5.92	5.84

heating and subsequent condensation into the membrane upon cooling.

To evaluate and compare alignment in various membranes, we generated curves of quadrupole splitting vs D_2O uptake for the three membranes in Figure 6. A comparison between splitting at similar D_2O uptakes reveals the relative degree of alignment. N112 exhibits the highest order among these membranes. In addition, this reproducible relationship enables one to conveniently characterize water uptake using the quadrupole splitting for a given membrane, once the splitting−uptake curve is established. As mentioned above, we are investigating

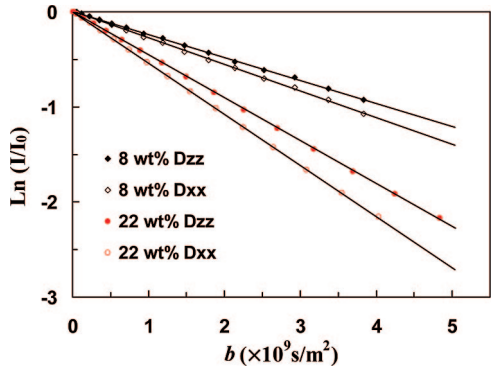

Figure 7. Normalized signal amplitudes (I/I_0) of stimulated echo decays vs Stejskal−Tanner parameter b for N112 with 8 and 22 wt % H_2O for a diffusion time $\Delta = 20$ ms at 25 °C. Solid symbols indicate signal decay for through-plane diffusion in the **z** direction D_{zz}. Open symbols indicate signal decay for in-plane diffusion in the **x** direction D_{xx}. Error bars are comparable to the data symbol size. The solid lines are linear least-squares one-component fits with correlation coefficients larger than 0.999.

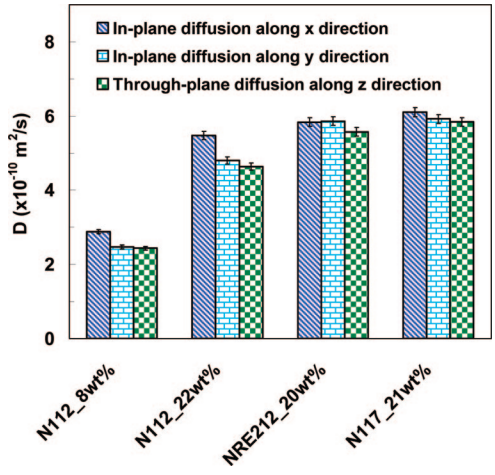

Figure 8. Water self-diffusion coefficients D at 25 °C measured by placing the water-swollen membranes at three angles with respect to the gradient direction. D values are averaged over a diffusion time Δ ranging from 7 to 50 ms. Error bars of ±2% indicate the accuracy of D measurements with respect to anisotropy (within each membrane group).

models of quadrupole splitting vs water uptake and channel order, which in this case might allow for extraction of the water channel cross section dependence as a function of water uptake.

B. Diffusion Anisotropy. The NMR stimulated echo signal decay I/I_0 is a function of b ($= \gamma^2 g^2 \delta^2 (\Delta - \delta/3)$, with dependence shown in Figure 7. We obtain self-diffusion coefficients D from the slopes of the fitted lines. It is evident that the slopes and therefore the diffusion coefficients for the same water-swollen N112 are different in through-plane (D_{zz}) and in-plane (D_{xx}, D_{yy} close in numerical value to D_{zz} not shown) directions. Here we note that D is in fact a tensor quantity, where our NMR measurements here determine the principal tensor components along the **x**, **y**, and **z** directions of the membranes by applying pulsed gradients along each direction separately. In Figure 8 we plot the water self-diffusion coefficients for water-swollen N112, NRE212, and N117 in three orthogonal directions. The gradient is parallel to $\mathbf{B}_0$; thus, we can use the same axis definitions **x**, **y**, **z** to indicate the diffusion direction with respect to the membrane orientation in the NMR coil. We varied diffusion time Δ from 7 ms to 50 ms to look for any morphological barriers that may cause tortuous diffusion[26] behavior. In all membranes, directions, temperatures, and water uptakes, the measured D values were stable over that range of diffusion times. A study of diffusion with smaller diffusion times Δ is underway to investigate morphological barriers (e.g., domain structure) on the ~1 μm scale. Figure 8 shows the average values for each case. These values are listed in Table 2 for easy comparison with orientational order measurements.

Clearly the self-diffusion of water in N112 at 22 wt % H_2O uptake in the extrusion direction (5.48×10^{-10} m^2/s) is 14% faster than in the perpendicular in-plane direction (4.81×10^{-10} m^2/s) and 18% faster than in the through-plane direction (4.64×10^{-10} m^2/s) This indicates that the energy barrier for water transport is lower in the direction in which the hydrophilic channels are aligned[2,3,27] and provides a substantial yet qualitative correlation with the above ^{2}H spectroscopic alignment measurements. At a lower water uptake of 8 wt %, the diffusion coefficients are smaller ($D_{xx} = 2.88 \times 10^{-10}$, $D_{yy} = 2.47 \times 10^{-10}$, $D_{zz} = 2.44 \times 10^{-10}$ m^2/s), but the ratio of D_{xx}/D_{zz} remains equal to 1.18, indicating the diffusion anisotropy is stable over a range of water uptake for a given membrane. The results for NRE212 and N117 show nearly isotropic diffusion behavior; i.e., diffusion coefficients are equal in all three directions within experimental error. This is probably due to the low degree of ordering in these two membranes. Though the alignment is discernible by ^{2}H NMR splitting, it is not high enough to lead to diffusion anisotropy. The small yet not quite significant differences for N117 and the biaxial N112 do follow the spectroscopic order measurements, while in NRE212, the small differences are at odds with the order measurements. We note that D in the extrusion direction of N112 approximates D for any direction in NRE212, while D's in the other two directions are slower than NRE212, giving the impression that diffusion is attenuated in the other two directions by the extrusion process. We believe that instead the overall channel connectivity (see below) of the NRE212 and N117 materials are higher than that

for N112, since they are processed and presumably chemically and thermally treated in different ways.

In addition to orientational order, the *connectivity* of the channels will also influence diffusion anisotropy as well as the magnitude of diffusion. For an average hydrophilic channel length, determined to be ~100 nm in XRD studies,[7,10] the water transport will certainly depend on how well the channels are interconnected. If an aligned morphology has more dead ends, then it will exhibit slower diffusion for water molecules along that direction. This may partially cancel out some of the diffusion enhancement effects induced by bulk alignment, which may be the case for NRE212. A morphological model possible for cast membranes such as NRE212 consists of long cylindrical channel bundles that are randomly oriented in-plane but have an average tilt angle toward the through-plane direction. This morphology would show average though-plane order, whereas the diffusion anisotropy will depend on the degree of the tilting. Through-plane diffusion would be faster or slower than that of in-plane due to extent of alignment (bundle tilt). A recent publication by Kidena showed diffusion anisotropy results for water in Nafion NRE-212CS and hydrocarbon ionomer membranes.[35] The author observed negligible diffusion anisotropy for NRE-212CS at room temperature, which is consistent with this study.

Note that we have thus far used the membranes "as is" without any attempt to induce order. We anticipate when the order is enhanced in a particular direction, the diffusion and proton conductivity in that direction should increase as well. We are beginning systematic spectroscopy and diffusion studies of membranes with enhanced alignment via various processes. For most fuel cell applications, high through-plane proton conductivity is desired, and our measurements point toward the need for increasing through-plane alignment and thus conductivity. However, Gruber et al. recently developed a lateral fuel cell[36] in which protons transport tangentially in the membrane plane. Such devices would benefit from higher in-plane proton conductivity, which is more easily achieved. Reports show that high-temperature annealing of extruded films produces increased fuel cell performance,[19,37] which might be explained due to randomization of alignment in these films, producing better through-plane conductivity than unannealed Nafion 112 films aligned in-plane. Furthermore, aging of membranes in operating fuel cells, which usually requires hours or days of operation before becoming stable,[19] could result from the evolution of flow alignment of the hydrophilic channels. These methods allow characterization of membrane order and diffusion properties of membrane ionomers before, after, or during device operation.

IV. Conclusions

We quantitatively measure bulk channel alignment in Nafion membranes using ^{2}H NMR directly on residually aligned absorbed D_2O. The numerical quantification of anisotropy properties such as the biaxiality parameter is straightforward using this method. We present results for three perfluorosulfonate ionomer membranes showing that the hydrophilic channels are biaxially oriented ($\eta = 0.12$) for extruded Nafion 112 membranes and uniaxially oriented for Nafion 117, both in the extrusion direction, whereas channels are uniaxially oriented perpendicular to the plane for dispersion-cast NRE212. These results show that water swelling (4−20 wt %) and thermal expansion (25−80 °C) for these membranes are affine, at least on the ~1 μm scale probed here by the ^{2}H quadrupole interaction. Water self-diffusion measurements demonstrate anisotropic transport in Nafion 112 with an in-plane diffusion coefficient 18% larger than that of through-plane at two hydration levels, while the anisotropic effect is minimal for Nafion 117 and NRE 212 due to lower order present in the latter two membranes.

This study represents the first direct comparison of a directional transport property (diffusion) with quantitative orientational order measurements for ionomer membranes. We are expanding these studies to include other membrane chemistries and morphologies in order to obtain a more complete picture of membrane transport and thus optimally design membranes for targeted applications. We propose that control over the direction and extent of orientational order of the hydrophilic channels will allow increased material design freedom and improvements in ionomer device performance, e.g., increased proton conductivity across the membrane plane in fuel cells.

Acknowledgment. This material is based upon work supported in part by the U.S. Army Research Office under Grant W911NF-07-1-0452 Ionic Liquids in Electro-Active Devices (ILEAD) MURI. Acknowledgment is made to the Donors of the American Chemical Society Petroleum Research Fund for partial support of this research and to Virginia Tech for startup funds. We also acknowledge Profs. James E. McGrath and Robert B. Moore and Dr. Abhishek Roy for helpful discussions and for providing N112 and N117 membrane samples.

References and Notes

(1) Mauritz, K. A.; Moore, R. B. *Chem. Rev.* **2004**, *104*, 4535–4585.
(2) Ma, S.; Siroma, Z.; Tanaka, H. *J. Electrochem. Soc.* **2006**, *153*, A2274–A2281.
(3) Cable, K. M.; Maurtiz, K. A.; Moore, R. B. *Chem. Mater.* **1995**, *7*, 1601–1603.
(4) Li, J.; Wilmsmeyer, K. G.; Madsen, L. A. *Macromolecules* **2008**, *41*, 4555–4557.
(5) Gierke, T. D.; Munn, G. E.; Wilson, F. C. *J. Polym. Sci., Part B: Polym. Phys.* **1981**, *19*, 1687–1704.
(6) Elliott, J. A.; Hanna, S.; Elliott, A. M. S.; Cooley, G. E. *Macromolecules* **2000**, *33*, 4161–4171.
(7) Rubatat, L.; Rollet, A. L.; Gebel, G.; Diat, O. *Macromolecules* **2002**, *35*, 4050–4055.
(8) Rubatat, L.; Gebel, G.; Diat, O. *Macromolecules* **2004**, *37*, 7772–7783.
(9) Elliott, J. A.; Paddison, S. J. *Phys. Chem. Chem. Phys.* **2007**, *9*, 2602–2618.
(10) Schmidt-Rohr, K.; Chen, Q. *Nat. Mater.* **2008**, *7*, 75–83.
(11) Chen, R. S.; Jayakody, J. P.; Greenbaum, S. G.; Pak, Y. S.; Xu, G.; McLin, M. G.; Fontanella, J. J. *J. Electrochem. Soc.* **1993**, *140*, 889–895.
(12) Rankothge, M.; Haryadi; Moran, G.; Hook, J.; Vangorkom, L. *Solid State Ionics* **1994**, *67*, 241–248.
(13) Xu, G.; Pak, Y. S. *Solid State Ionics* **1992**, *50*, 339–343.
(14) McLean, R. S.; Doyle, M.; Sauer, B. B. *Macromolecules* **2000**, *33*, 6541–6550.
(15) Burnell, E. E.; De Lange, C. A. *NMR of Ordered Liquids*; Kluwer: Dordrecht, 2003.
(16) Deloche, B.; Samulski, E. T. *Bull. Am. Phys. Soc.* **1981**, *26*, 327–328.
(17) Callaghan, P. T.; Samulski, E. T. *Macromolecules* **2003**, *36*, 724–735.
(18) Yu, L. J.; Saupe, A. *Phys. Rev. Lett.* **1980**, *45*, 1000–1003.
(19) Zhao, T. S.; Kreuer, K.-D.; Nguyen, T. V. *Advances in Fuel Cells*; Elsevier: Amsterdam, 2007; Vol. *1*.
(20) Lee, J. H.; Nam, J. D.; Choi, H.; Jung, K.; Jeon, J. W.; Lee, Y. K.; Kim, K. J.; Tak, Y. *Sens. Actuators, A* **2005**, *118*, 98–106.
(21) Shoji, E.; Hirayama, D. *J. Phys. Chem. B* **2007**, *111*, 11915–11920.
(22) Zawodzinski, T. A.; Neeman, M.; Sillerud, L. O.; Gottesfeld, S. *J. Phys. Chem.* **1991**, *95*, 6040–6044.
(23) Saito, M.; Arimura, N.; Hayamizu, K.; Okada, T. *J. Phys. Chem. B* **2004**, *108*, 16064–16070.
(24) Thampan, T.; Malhotra, S.; Tang, H.; Datta, R. *J. Electrochem. Soc.* **2000**, *147*, 3242–3250.
(25) Paddison, S. J.; Paul, R.; Zawodzinski, T. A. *J. Electrochem. Soc.* **2000**, *147*, 617–626.
(26) Zhang, J. H.; Giotto, M. V.; Wen, W. Y.; Jones, A. A. *J. Membr. Sci.* **2006**, *269*, 118–125.
(27) Gardner, C. L.; Anantaraman, A. V. *J. Electroanal. Chem.* **1998**, *449*, 209–214.
(28) Silva, R. F.; De Francesco, A.; Pozio, A. *J. Power Sources* **2004**, *134*, 18–26.

(29) Fechete, R.; Demco, D. E.; Blumich, B. *Macromolecules* **2003**, *36*, 7155–7157.
(30) Rollet, A. L.; Diat, O.; Gebel, G. *J. Phys. Chem. B* **2004**, *108*, 1130–1136.
(31) Stejskal, E. O.; Tanner, J. E. *J. Chem. Phys.* **1965**, *42*, 288–292.
(32) Madsen, L. A.; Dingemans, T. J.; Nakata, M.; Samulski, E. T. *Phys. Rev. Lett.* **2004**, *92*, 145505.
(33) Severing, K.; Saalwachter, K. *Phys. Rev. Lett.* **2004**, *92*, 125501.
(34) Geary, J. M.; Goodby, J. W.; Kmetz, A. R.; Patel, J. S. *J. Appl. Phys.* **1987**, *62*, 4100–4108.
(35) Kidena, K. *J. Membr. Sci.* **2008**, *323*, 201–206.
(36) Gruber, K.; Loibl, H.; Schlauf, T.; Pallanits, J.; Gornik, C.; Kronberger, H.; Fafilek, G.; Nauer, G. *Electrochem. Commun.* **2007**, *9*, 1288–1292.
(37) Hensley, J. E.; Way, J. D.; Dec, S. F.; Abney, K. D. *J. Membr. Sci.* **2007**, *298*, 190–201.

MA802106G